ADVANCED HEALTHCARE MATERIALS
www.advhealthmat.de

Sustained Release of Human Adipose Tissue Stem Cell Secretome from Star-Shaped Poly(ethylene glycol) Glycosaminoglycan Hydrogels Promotes Motor Improvements after Complete Transection in Spinal Cord Injury Rat Model

Deolinda Silva, Lucas Schirmer, Tiffany S. Pinho, Passant Atallah, Jorge R. Cibrão, Rui Lima, João Afonso, Sandra B-Antunes, Cláudia R. Marques, João Dourado, Uwe Freudenberg, Rui A. Sousa, Carsten Werner, and António J. Salgado**

Adipose tissue-derived stem cells (ASCs) have been shown to assist regenerative processes after spinal cord injury (SCI) through their secretome, which promotes several regenerative mechanisms, such as inducing axonal growth, reducing inflammation, promoting cell survival, and vascular remodeling, thus ultimately leading to functional recovery. However, while systemic delivery (e.g., i.v. [intravenous]) may cause off-target effects in different organs, the local administration has low efficiency due to fast clearance by body fluids. Herein, a delivery system for human ASCs secretome based on a hydrogel formed of star-shaped poly(ethylene glycol) (starPEG) and the glycosaminoglycan heparin (Hep) that is suitable to continuously release pro-regenerative signaling mediators such as interleukin (IL)-4, IL-6, brain-derived neurotrophic factor, glial-cell neurotrophic factor, and beta-nerve growth factor over 10 days, is reported. The released secretome is shown to induce differentiation of human neural progenitor cells and neurite outgrowth in organotypic spinal cord slices. In a complete transection SCI rat model, the secretome-loaded hydrogel significantly improves motor function by reducing the percentage of ameboid microglia and systemically elevates levels of anti-inflammatory cytokines. Delivery of ASC-derived secretome from starPEG-Hep hydrogels may therefore offer unprecedented options for regenerative therapy of SCI.

1. Introduction

Spinal cord injury (SCI) has been known as "an ailment not to be treated" since ancient Egyptian times, about 2500 years before the common era (B.C.E).[1] However, even thousands of years later, no effective cure exists. SCI incidence is ≈54 cases per one million people or about 17 700 new cases per year in the United States alone.[2] As a severely disabling condition, SCI encompasses a detrimental impact on the quality of life of patients afflicted. The disease affects both motor and sensory functions in the body. Although physical disabilities are the major incapacitating alterations, patients are further burdened by the emerging psychological and financial concerns.[3,4]

SCI pathophysiology comprehends three main phases: the primary injury starts when a mechanical impact compresses, contuses, or lacerates the spinal cord, disrupting ascending and descending tracts.[5] Massive amounts of inflammatory cells infiltrate injured tissue, leading to the release of pro-inflammatory cytokines

D. Silva, T. S. Pinho, J. R. Cibrão, R. Lima, J. Afonso, S. B-Antunes, C. R. Marques, J. Dourado, A. J. Salgado
Life and Health Sciences Research Institute (ICVS), School of Medicine University of Minho
Campus de Gualtar, Braga 4710-057, Portugal
E-mail: asalgado@med.uminho.pt

D. Silva, T. S. Pinho, J. R. Cibrão, R. Lima, J. Afonso, S. B-Antunes, C. R. Marques, J. Dourado, A. J. Salgado
ICVS/3B's – PT Government Associated Laboratory
Braga/Guimarães 4710-057, Portugal

The ORCID identification number(s) for the author(s) of this article can be found under https://doi.org/10.1002/adhm.202202803

DOI: 10.1002/adhm.202202803

D. Silva, T. S. Pinho, S. B-Antunes, R. A. Sousa
Stemmatters, Biotecnologia e Medicina Regenerativa SA
Zona Industrial da Gandra, Barco, Guimarães 4805-017, Portugal

L. Schirmer, P. Atallah, U. Freudenberg, C. Werner
Leibniz Institute of Polymer Research Dresden (IPF)
Max Bergmann Center of Biomaterials Dresden (MBC)
01069 Dresden, Germany
E-mail: werner@ipfdd.de

C. Werner
Center for Regenerative Therapies Dresden (CRTD)
Technische Universität Dresden
Fetscherstraße 105, 01307 Dresden, Germany

initiating the second phase.[6] In addition, cell death and damage to spinal neurons and axons also occur.[5,7] A chronic or third phase is then established, with a cystic cavity formed and surrounded by reactive astrocytes. Furthermore, the demyelination of white matter together with grey matter dissolution creates an inhibitory environment for the regenerative process.[8] The complexity of this cascade of events makes developing regenerative approaches for SCI far more complex when compared to other trauma-related injuries.

Cell-based therapies have opened a window of new possible therapeutic approaches that have been studied in both preclinical models and clinical applications.[9–12] In particular, adipose tissue-derived stem cells (ASCs) can provide protection, survival, and differentiation of neural cells and support neuroregeneration with their beneficial immunomodulatory profile.[13–15] In addition, the implantation of ASCs in a contusion mice model enhanced functional recovery, reduced inflammation, and preserved neural tissue.[10] Moreover, our group showed that the transplantation of a combination of ASCs and olfactory ensheathing cells (OECs) within a gellan gum hydrogel improved motor function by reducing inflammatory cells in the lumbar[16] and thoracic hemisection SCI rat model.[9] Likewise, this approach was capable of increasing diaphragmatic activity and partially restoring sensory function in cervical level 2 (C2) hemisection SCI in rats.[17]

The impact of cell transplantation on regenerative processes is mainly conveyed through their secreted bioactive molecules (secretome), including soluble proteins (cytokines, growth factors, and chemokines) and a vesicular fraction (exosomes), both of which have neuroprotective, neuroregenerative, and immunomodulatory capabilities.[13,18] Thus, ASCs-derived secretome has been shown to protect pheochromocytoma (PC12) cells from glutamate excitotoxicity and apoptosis by reducing the levels of cleaved-caspase-3.[14] Regarding inflammation, the ASCs secretome is able to reduce the release of pro-inflammatory tumor necrosis factor-α (TNF-α) after exposure to an inflammatory stimulus, as well as to induce active macrophages (M2) polarization and the secretion of anti-inflammatory cytokines IL-10 and transforming growth factor (TGFβ1).[19] Furthermore, the ASCs secretome was shown to be capable of promoting neuronal survival and differentiation,[20,21] axonal outgrowth in dorsal root ganglia (DRG) explants,[9,22] and also tissue vascularization.[23]

Based on these positive effects on neuroregeneration, our group recently showed that ASCs secretome can promote functional recovery in an SCI mice model by multiple systemic injections.[24] The beneficial effects have only been observed by systemic administration in this study, whereas the action of local injection was greatly diminished due to its quick clearance of the secretome from the target site. However, systemic administration also presents some disadvantages, frequently associated with rapid diffusion through the body and off-target effects.[25] Other strategies involve catheter implantation or mini pumps, which come with the downside of the additional risk of infections at the delivery site.[26,27]

Taking all of the previous into account, new methods of sustained administration must be developed, such as hydrogels. Indeed, in recent years several studies have demonstrated the ability of hydrogels to serve as delivery platforms for a variety of therapeutic agents for a plethora of disabled conditions. In an SCI rat model, elastic poly(sebacoyl diglyceride) coated with isoleucine-lysine-valine-alanine-valine-serine hydrogel loading neural stem cells promoted improved motor function while reducing inflammation and cell death.[28] Pan and coworkers also demonstrated that the release of human periodontal ligament stem cells from a thermosensitive hydrogel overexpressing platelet-derived growth factor-BB (PDGF-BB) supported bone regeneration.[29] Hydrogels have also been identified as promising candidates for chemotherapeutic drug delivery as an alternative to conventional methods.[30] Overall, these findings strongly support the development and application of hydrogels as delivery systems. In fact, the ability of hydrogels to act as release systems is directly related to their ability to integrate at lesion sites, support tissue regeneration, and load and release a wide range of small molecules or biological compounds.[31–34] In particular, the viscoelasticity, cell compatibility, and biofunctionalization of hydrogels can support the treatment of SCI.[35]

Poly(ethylene glycol) (PEG) is a biocompatible synthetic polymer that has been widely used to design hydrogels that allow axonal growth, vascularization, infiltration of glial cells;[36] promote functional recovery, and reduce cystic cavity.[37] Moreover, these hydrogels can be easily functionalized with cell-instructive peptides, such as Arg-Glys-Asp (RGD), to improve cell loading and survival.[38] The physical and chemical characteristics of PEG-based hydrogels, such as their inert characteristics avoiding interactions with proteins, are favorable to create a permissive environment to drive the diffusion of molecules which confers an advantage of using them as encapsulating platforms.[39] For instance, the controlled delivery of brain-derived neurotrophic factor (BDNF) and glial-derived neurotrophic factor (GDNF) from PEG-based hydrogels into the brain has been beneficial to reduce microglial response[40] as the local delivery of neurotrophin-3 (NT-3) in SCI induced axonal growth and functional recovery,[32] corroborating the potential of these hydrogels as delivery systems.

However, hydrogels lacking affinity sites for cytokines and growth factors can hardly provide long term release. To overcome this limitation, biohybrid hydrogels made of starPEG (star-shaped PEG) and the glycosaminoglycan (GAG) heparin (Hep) have been produced and demonstrated to enable the sustained release of various growth factors.[41–43] In this system, the anionic charge arising from the high density of sulfate moieties on heparin results in a high affinity for a broad range of growth factors, cytokines, and chemokines mainly due to electrostatic interactions.[44] This effect has been previously utilized to modulate the release of multiple growth factors such as FGF-2 and vascular endothelial growth factor (VEGF)[45] or cytokines, such as IL-4[46] in a controlled and sustained manner over weeks. Additionally, these matrices can be applied as in situ forming hydrogels, which allow for the injection in a liquid state at the injury site, and posterior fast polymerization due to a Michael type reaction.[47]

Herein, we draw benefit from the high concentration of binding sites within a customized starPEG-Heparin (starPEG-Hep) hydrogel for controlled release of human ASCs (hASCs) secretome consisting of an effective combination of different growth factors and cytokines. Fluorescein isothiocyanate (FITC) labeled secretome and membrane-based protein arrays were used to assess the cumulative release of the secretome from starPEG-Hep

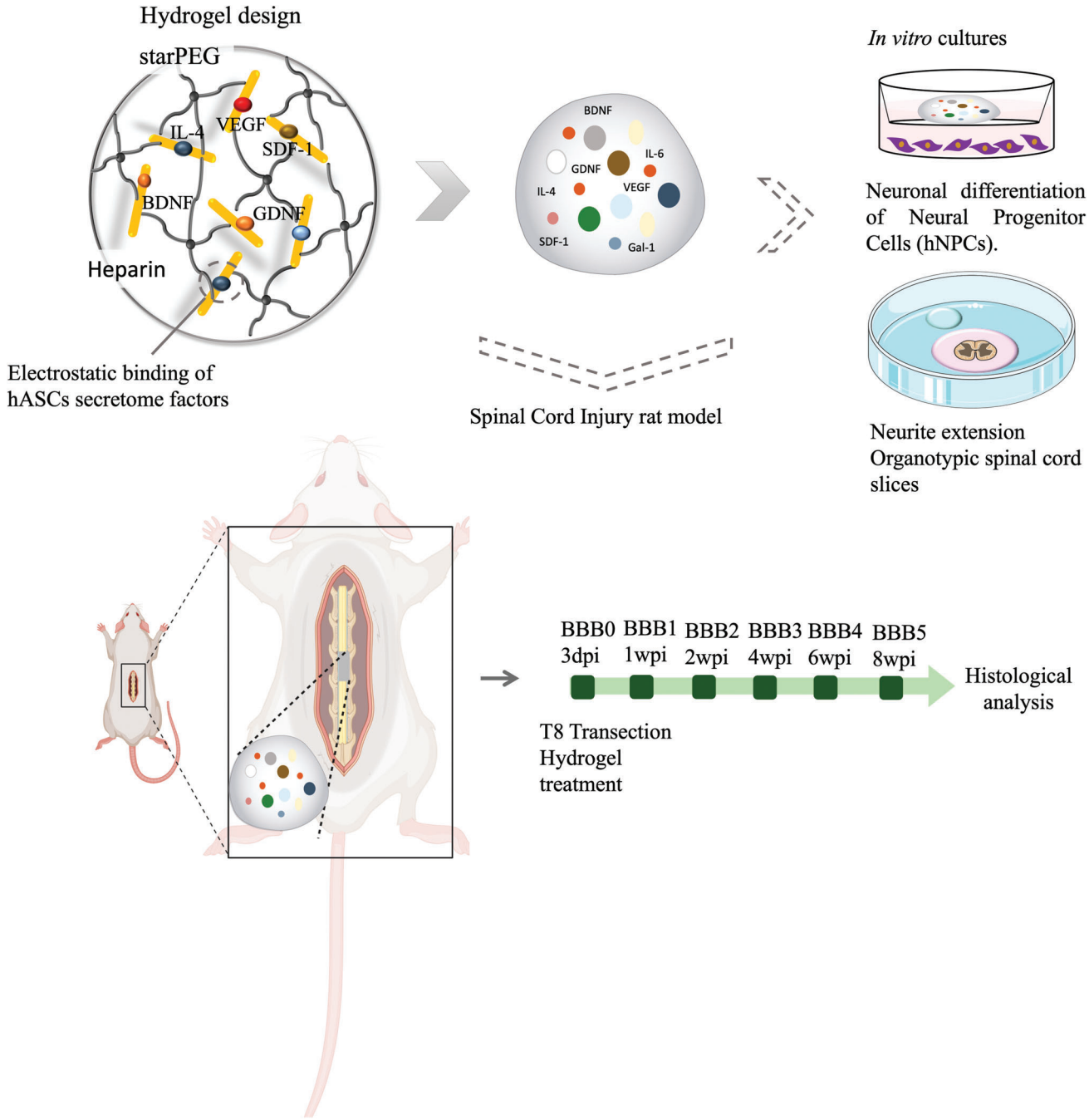

Figure 1. Schematic representation of our biomaterial concept, in vitro cultures, and in vivo model that were used to evaluate the bioactivity of human adipose-tissue derived stem cells (hASCs) secretome released from starPEG-Hep hydrogels. StarPEG-Hep hydrogels are formed by Michael type addition between thiol-terminated 4-arm starPEG and maleimide-functionalized heparin. Through electrostatic interactions, signaling mediators of the hASCs secretome bind to heparin to enable a controlled and sustained release. Bioactivity of released secretome was evaluated by the capacity to promote neuronal differentiation of human neural progenitor cells (hNPCs) and organotypic spinal cord cultures. In a final assessment, recovery of thoracic (T8) level transected rats by secretome-loaded starPEG-Hep hydrogels was analyzed.

hydrogels. In vitro bioactivity was evaluated in the capacity to induce neuronal differentiation in human neural progenitor cells (hNPCs) and neurite growth in organotypic spinal cord slices. Finally, this release system's potential to promote regeneration after a complete transection in an SCI rat model was assessed (**Figure 1**).

2. Results and discussion

2.1. Physical Characterization of In Situ Forming Hydrogels

StarPEG-GAG hydrogels have been well characterized regarding their mechanical as well as biomolecular behavior and

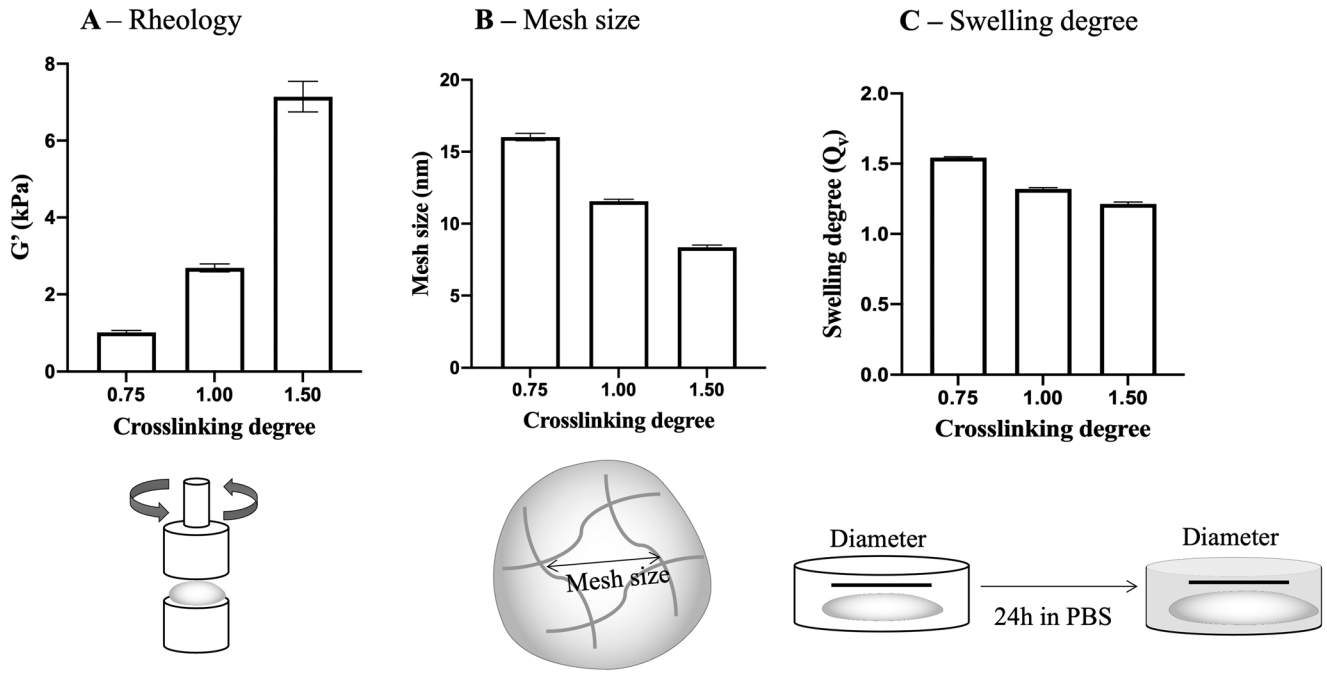

Figure 2. Physical characterization of starPEG-Hep hydrogels. At different crosslinking degrees (starPEG/Hep molar ratio) hydrogels characteristics such as A) stiffness, B) mesh size (calculated based on rubber elasticity theory,[41,56] and C) swelling degree, were measured. Hydrogels can vary from soft to stiff materials, decreasing mesh size and swelling degree upon increasing crosslinking degree. Measurements are plotted as mean ± SEM, corresponding to 9 replicates.

have previously been presented as a suitable matrix for in vivo implantation.[41,48,49] These hydrogels are formed from heparin functionalized with six maleimide groups together with thiol-terminated, 4-arm starPEG. The physical properties of the hydrogels can be adjusted by the number of starPEG molecules reacting with heparin maleimide groups, changing the degree of crosslinking, thus modulating the stiffness, mesh size, and swelling.[47,50] Increasing the crosslinking degree from 0.75 to 1 and 1.5, hydrogels increase their storage modulus from 1.01 ± 0.13 to 2.69 ± 0.30 to 7.14 ± 0.97 kPa, respectively (**Figure 2**A), ranging from soft to stiff materials. This control over material stiffness is highly important in SCI, where the material's mechanical properties should mimic the spinal cord's soft tissue.[51] In this manner, the low stiffness hydrogels were selected to be used in this work, mainly due to its similar stiffness to neuronal tissue and its ability to allow axons to grow throughout the material.[52] Furthermore, mesh size and swelling degree decrease with increased crosslinking degree (Figure 2B,C, Table S1, Supporting Information). The mesh size will allow the diffusion of molecules through the material.[53] Hydrogels injected at the spinal cord may swell around twice the initial volume to avoid additional pressure or lesion in the tissue.[54,55] In accordance, starPEG-Hep hydrogels have a low swelling degree, between 1.2 and 1.5, which will ensure no damage to the tissue.

2.2. Characterization of Secretome Released from starPEG-Hep Hydrogels

In the context of SCI, administering a therapy is still a concern, considering the administration route and associated problems, such as toxic side effects promoted by high doses or the rapid clearance by the fluids at the injury site. Moreover, the enzymatic degradation at the injury site can compromise the bioactivity of drugs and molecules.[57] To minimize these problems, starPEG-GAG hydrogels can be easily integrated at the lesion site and bind, protect, and sustainable deliver the secretome of ASCs. As the secretome of ASCs has already been characterized to be composed of a wide range of signaling factors,[21,58,59] our approach capitalizes from the high number of binding sites within the starPEG-Hep hydrogels that allow for independent release of multiple factors[42] and thus should be a promising choice for delivering hASCs secretome within SCI sites. Several release assays were conducted to evaluate the release profile of the hASCs secretome from starPEG-Hep hydrogels. In a first approach, the secretome was labeled with a FITC dye that binds to amine groups of proteins, enabling their detection by fluorescence intensity. Then, the labeled secretome was loaded into starPEG-Hep hydrogels with an efficiency of immobilization of about 95% and incubated in phosphate buffered saline (PBS) with 1% bovine serum albumin (BSA). To characterize the release of the secretome, samples from the supernatant that have been in contact with the hydrogel were collected over 10 days, revealing a controlled and prolonged release profile (**Figure 3**A). Briefly, after a burst release during the first day (≈45%) the hydrogel showed a cumulative release of the secretome until 10 days, reaching ≈70% of release at that time point of the experiment. Over the following 9 days, a sustained release of the secretome was detected.

These results show the hydrogel's potential as a sustained release system for the secretome. In order to elucidate more closely

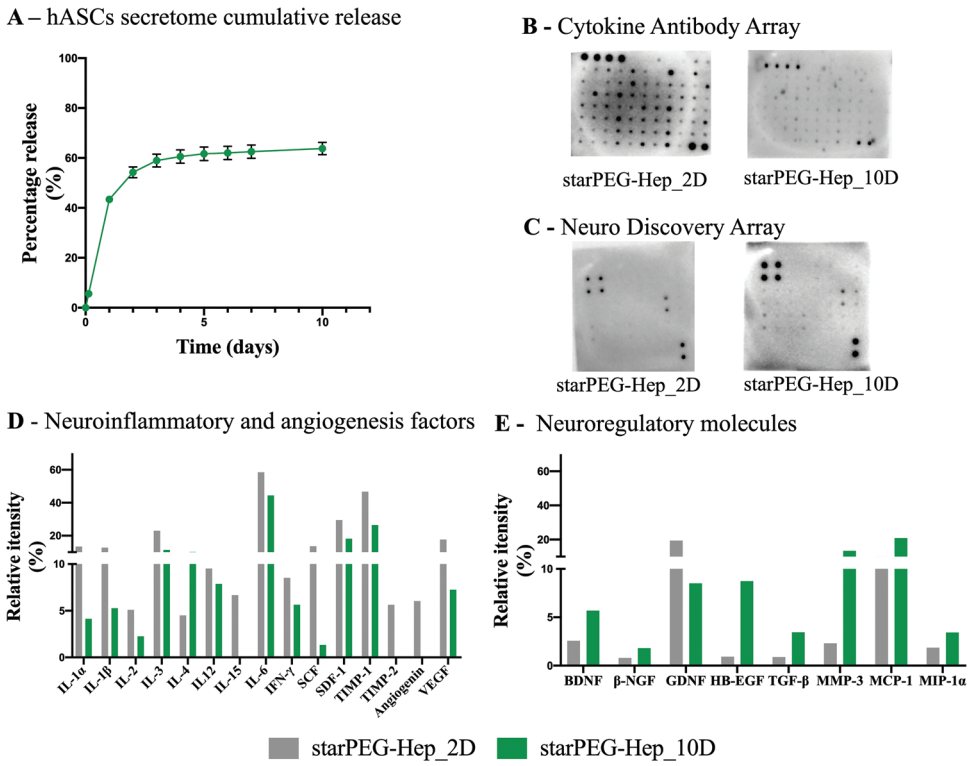

Figure 3. Characterization of hASCs secretome release from starPEG-Hep hydrogels. A) FITC-labeled secretome was loaded to starPEG-Hep hydrogels and samples were collected at 0, 3 h, 1, 2, 3, 4, 5, 6, 7, and 10 days. Secretome was detected by fluorescence and the cumulative release was calculated over time. Values are plotted as mean ± SEM from two independent experiments with seven replicates. To decipher which molecules were being released from starPEG-Hep hydrogels, a membrane based-protein array was performed of samples collected at 2 and 10 days. B,C) show the membranes of Cytokines Antibody arrays and Neuro Discovery arrays, respectively. D) Relative intensity of factors involved in neuroinflammatory and angiogenesis, such as IL-4, tissue inhibitor of metalloproteinase (TIMP)-1, and VEGF, present a higher release in the first 2 days. E) On the opposite neuroregulatory molecules like BDNF, β-NGF, or TGF-β are mainly released within 2–10 days of release. Values are presented as relative intensity, in percentage, for the positive control in each membrane.

which components of the secretome were being released from starPEG-Hep hydrogels, membrane-based protein arrays were used. Membrane-based protein arrays detect multiple protein levels with high sensitivity and specificity in a single experiment. The technology is based on the sandwich immunoassay, in which each dot in the membrane represents a single factor and signals are detected using chemiluminescence (Figure 3B,C).[60] For this purpose, samples of released secretome were collected only at 2 and 10 days and evaluated separately using Human Neuro Discovery Array C1 and Human Cytokine Antibody Array C5 (Figure 3B–E), allowing the detection of known ASCs released neurotrophic factors and cytokines after 2 days and 2–10 days, respectively. This allows to determine whether all factors are released after 2 days or if they are delayed until the end of the experiment. This could also be useful in determining which processes are being addressed by the protein release for biological purposes. Each dot was quantified and normalized to the positive controls to determine the relative amount released at different time points. Membrane arrays revealed a different release profile of neuroinflammatory and angiogenic factors (Figure 3D) compared with neuroregulatory molecules (Figure 3E). In fact, cytokines that play a role in modulating the immune response, such as IL-1α, IL-1β, IL-2, IL-3, and IL-4, or factors involved in angiogenesis like angiogenin or VEGF had a burst release after 2 days. Despite that, the cumulative release observed after 10 days evidenced their continuous and extended release. In contrast, growth factors that promote neuronal growth and survival like BDNF, β-NGF, heparin binding epidermal growth factor are mainly released within 2–10 days, indicating overall an instant release of immune modulating factors and a slightly delayed but therefore more prolonged release of neuro-regulating factors. Moreover, it was possible to detect a wide range of molecules present in the secretome of hASCs that were continuously released from the hydrogels such as fibroblast growth factor (FGF), transforming growth factor beta (TGF-β), hepatocyte growth factor, NT-3, NT-4, IL-16 (Figures S1 and S2, Supporting Information). Altogether, these results support and explain the cumulative release profile presented in Figure 3A. While Figure 3A shows the total release of the secretome, membrane-based protein arrays show which of these factors are released over time. The burst release results from high amounts of neuroinflammatory and angiogenic factors released in the first days, while the continuous and prolonged release until 10 days is driven mainly by neuroregulatory growth factors. This pattern may also indicate the different affinity of various proteins to heparin which control the overall release characteristics.[61] This profile is in line with other approaches that used hydrogels as affinity-based delivery systems incorporating heparin to deliver fibroblast growth factor (FGF-2),[34,62] and

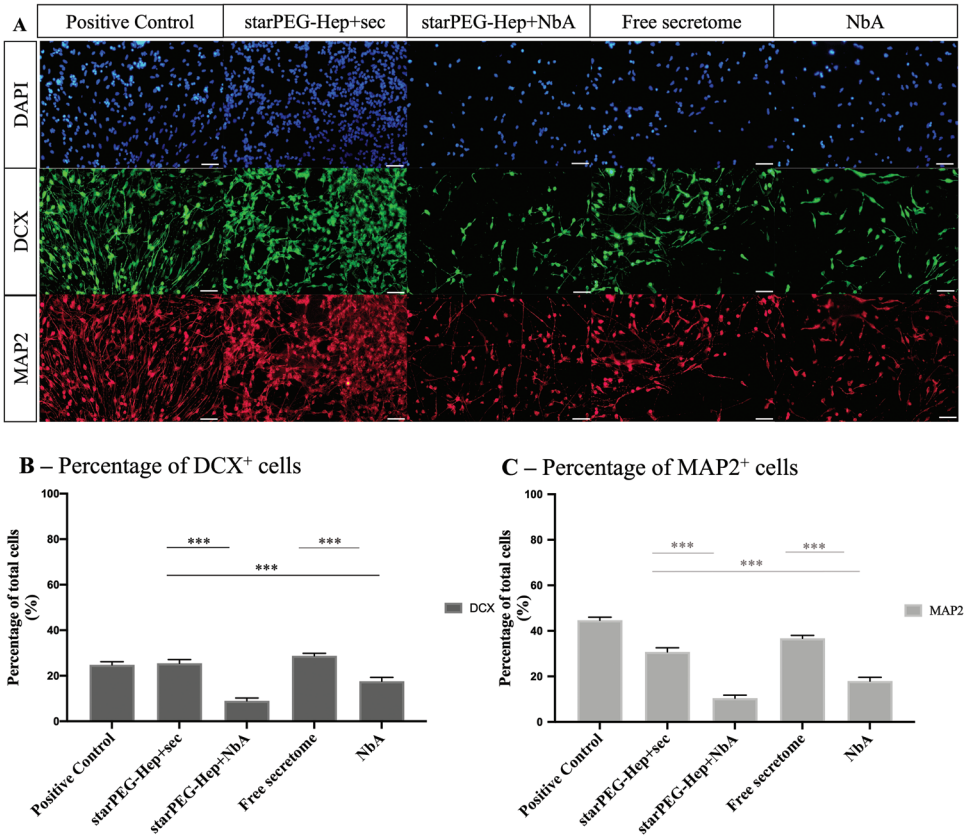

Figure 4. Effect of hASCs secretome released from starPEG-Hep hydrogels on hNPCs differentiation in vitro. A) Representative micrographs of hNPCs differentiation in immature (DCX) and mature (MAP2) neurons when exposed to control, secretome- or vehicle in which secretome was collected (NbA)-loaded starPEG-Hep hydrogels, free secretome or NbA conditions. Nuclei are stained with DAPI and neurons with anti-MAP2 and anti-DCX. B,C) Quantification of the percentage of DCX^+, $MAP2^+$ cells from total cells, respectively. Results are representative of two independent experiments with 8/12 replicates in a total of ten representative fields per replicate. Mixed ANOVA; ***$p < 0.0001$. Error bars represent mean ± SEM. Scale bar: 50 µm. MAP2 microtubule-associated protein 2, DCX doublecortin, DAPI 4′,6′-diamino-2-fenil-indol.

was effective in promoting their prolonged release and improved functional recovery after SCI in animal models.

2.3. hASCs Secretome Released from starPEG-Hep Hydrogels Promotes Differentiation of hNPCs and Neurite Outgrowth in Organotypic Cultures

Testing of the bioactivity of the developed hydrogel system then followed through the evaluation of the differentiation of hNPCs. For this goal, hNPCs were seeded as a single monolayer of adherent cells on precoated coverslips with poly-D-Lysin and laminin, after which secretome-loaded starPEG-Hep (starPEG-Hep+sec) hydrogels were placed in an insert above the cell layer. After 5 days in culture, differentiation of hNPCs was assessed by immunocytochemistry (ICC) analysis for doublecortin positive cells (DCX^+) and microtubule-associated protein positive cells ($MAP2^+$), staining immature and mature neurons, respectively. Fluorescence microscopy images showed hNPCs differentiation (**Figure 4**A). Statistical analysis showed that there was an effect of factor treatment (F (4,474) = 57.87, $p < 0.0001$, $\eta^2_{partial} = 0.33$), and the differentiation condition (F (1,474) = 153.66, $p < 0.0001$, $\eta^2_{partial} = 0.25$), and the interaction between these two factors (F (4,474) = 40.15, $p < 0.0001$, $\eta^2_{partial} = 0.25$). As shown in Figure 4B, hASCs secretome released from starPEG-Hep hydrogels presented significative higher percentage of DCX^+ cells when compared with hydrogel loading the vehicle in which secretome was collected (Neurobasal A) (starPEG-Hep+NbA) (n = 120; 25.47 ± 17.90 versus n = 99; 9.08 ± 12.66; $p < 0.0001$) or the vehicle alone (n = 80; 17.57 ± 15.37; $p < 0.0001$). No statistical differences were observed compared with the positive control (n = 100; 24.77 ± 13.87; $p = 0.72$) or free secretome ($n = 80$; 28.78 ± 9.97; $p = 0.11$), which was in contact with cells for the entire experiment. The same tendency is observed regarding the staining of mature neurons ($MAP2^+$). Cells treated with secretome released from starPEG-Hep hydrogels promoted a higher differentiation of $MAP2^+$ cells (Figure 4C) compared to cells treated with the vehicle released from the hydrogel (n = 120; 30.75 ± 19.80 versus n = 99; 10.43 ± 13.23; $p < 0.0001$) and cells treated only with vehicle (n = 80; 17.95 ± 15.01; $p < 0.0001$). Significance was also observed when comparing with positive control (n = 100; 44.78 ± 13.34; $p < 0.0001$) or free secretome ($n = 80$; 36.72 ± 11.74; p = 0.007). All statistical values are presented in Table S2, Supporting Information.

With this, we have shown that starPEG-Hep hydrogels are suitable for sustainably releasing a wide range of molecules, that

are closely implicated in regenerative processes such as BDNF and NGF, which are known to be involved in the survival, proliferation, and differentiation of hNPCs through the extracellular signal-regulated kinase (ERK) pathway.[63,64] Additionally, TIMP-1, highly released by starPEG-Hep+sec hydrogels, is also involved in the differentiation of oligodendrocyte progenitor cells (OPCs) by activating the protein kinase B (Akt) pathway.[65] These results are also in line with our previous work, where we showed the effects of hASCs secretome in inducing proliferation and metabolic activity of hippocampal neurons,[66] promoting differentiation of hNPCs and neurite outgrowth of DRG explants.[22] The secretome's role in modulating regenerative processes may rely on initial inflammatory activity created by the early release of pro-inflammatory cytokines, such as IL-1α, IL-1β or IL-2 (Figure 3D), which are required to activate elements of innate response and may be involved in the proliferation and differentiation of reparative cells.[67,68] On the other hand, the time-dependent release of anti-inflammatory cytokines, IL-10, and pro-regenerative molecules such as BDNF, NGF, or even TGF-β (Figure 3E) helps to restrict the immune response while also triggering axonal sprouting and regeneration.[69]

Given the generally low neuroregenerative capacity observed in SCI, it is of the utmost importance to develop therapies that can promote better regeneration. Bearing this in mind, organotypic spinal cord slice cultures were used as a more representative assay to evaluate the potential of hASCs secretome in promoting axonal or neurite outgrowth. After 7 days in culture, the secretome effect was evaluated by staining slices with neurofilament (NF) antibody (**Figure 5**). Quantification was performed by normalizing the total area occupied by the neurite to the total slice area. Statistical analysis evidenced the effect of the treatment (F (3.65) = 12.22, $p < 0.001$). Indeed, as shown in Figure 5B the percentage of relative NF area was significantly higher in the presence of starPEG-Hep+sec when compared with starPEG-Hep+Nb ($n = 16$; 25.70 ± 12.04 versus $n = 17$; 18.04 ± 8.47; $p = 0.039$). Statistical significance was also detected when compared with the control group ($n = 19$; 12.73 ± 2.58; $p < 0.001$) and to free secretome ($n = 17$; 10.71 ± 5.72; $p < 0.001$, Table S3, Supporting Information). The observed effect of hASCs secretome in promoting neurite outgrowth can be attributed to the released signaling mediators, such as BDNF, which induces outgrowth of cortical and hippocampal neurons[70] as well as supports axonal growth.[71] Neurite extension in organotypic spinal cord slices could be caused by the growth factors released during the first days, such as GDNF, FGF-2, and NT-3 supporting neurogenesis, axonal growth, and cell metabolism.[64,72,73] However main effects may be most likely governed by factors released from 2–10 days, such as BDNF and NGF, as the medium was changed after 48 h, in an attempt to recapitulate the rapid clearance by the fluid at the SCI lesion site.[74] Other highly released factors can also influence these processes, such as IL-6, which can enhance sprouting and functional recovery, as observed in lesioned hippocampal slices associated with a high level of growth associated protein (GAP)-43 expression, a protein associated with axonal growth,[75] or by activating mitogen-activated protein kinase (MAPK) signaling pathway inducing regeneration.[76] Apart from specific well-known molecules related to the beneficial effects of the secretome in in vitro and in vivo cultures, stomal cell-derived factor (SDF)-1, previously shown to be sustainably released from starPEG-Hep hydrogels,[77] has been associated with tissue protection, namely when mesenchymal stem cells (MSCs) overexpress this factor after myocardial infarction leading to the preservation of cardiac tissue.[78]

Altogether, these results emphasize the potential of starPEG-Hep hydrogels as a release system for a broad spectrum of the neuroregenerative signaling mediators of the hASCs secretome that can induce neural differentiation and neurite outgrowth. Furthermore, the promising avenue in promoting an extended release of secretome from starPEG-Hep hydrogels holds up not only for the action of single factors, but most likely for the balance between pro-inflammatory and pro-regenerative factors that are being released in an optimal time-dependent frame that favor the processes of regeneration path, when compared with free secretome condition.

2.4. hASCs Secretome Released from starPEG-Hep Hydrogels Promotes Motor Recovery in an SCI Animal Model

The secretome of hASCs has previously been shown to induce regeneration after SCI in animal models.[24,79] Herein, we aimed to develop a hydrogel system capable of controlled and prolonged release of secretome at the injury site to potentiate its effect. Considering the pro-regenerative capacity shown on hNPCs and spinal cord slices within the in vitro studies, we explored the potential of the released secretome in promoting motor improvements after a complete transection in a rat model. Animals were divided into five groups: SCI treated with starPEG-Hep+sec ($n = 7$); SCI treated starPEG-Hep+NbA ($n = 4$); SCI treated with secretome locally ($n = 7$); SCI treated with NbA ($n = 6$); and non-injured animals (laminectomy—SHAM group; $n = 7$). Complete transection was performed at T8 level, which resulted in a very severe lesion compared with hemisection or contusion models.[80] Animals were immediately treated and motor recovery was evaluated every 2 weeks until 8 weeks post-injury by Basso, Beattie, and Bresnahan (BBB) test.

Animals treated with starPEG-Hep+sec displayed improved motor outcomes compared with other groups (**Figure 6**). In addition, SHAM animals did not present motor deficits during that time. Statistical analysis revealed an effect of factor time (weeks F (5,130) = 33.54 $p < 0.0001$, $\eta^2_{\text{partial}} = 0.56$), and treatment ($F$ (4,26) = 948.54 $p < 0.0001$, $\eta^2_{\text{partial}} = 0.99$) and the interaction between these two factors (F (20,130) = 3.90 $p < 0.0001$, $\eta^2_{\text{partial}} = 0.38$). In particular, the mean BBB score was significantly improved by starPEG-Hep+sec treatment at 2, 6, and 8 weeks post-injury (wpi). Moreover, at 2 and 6 wpi, animals treated with starPEG-Hep+sec showed improved motor function when compared with animals treated with only secretome (2 wpi: 2 ± 2 versus 0.71 ± 0.57; $p = 0.032$; 6 wpi: 3.5 ± 2.25 versus 1.29 ± 0.95; $p = 0.004$). Notably, at 8 wpi animals treated with starPEG-Hep+sec showed statistically significant improvements compared with starPEG-Hep+NbA (4.07 ± 2.24 versus 2.00 ± 0.82; $p = 0.012$), animals treated with only secretome (1.86 ± 0.85, $p = 0.002$) and animals lesioned treated with vehicle (2.25 ± 0.69; $p = 0.013$). Interestingly, comparing the group treated with starPEG-Hep+sec with free secretome, a difference of approximately two points in BBB scale was reported clearly showing a beneficial effect of the hydrogel-based release. Furthermore, this is consistent with our

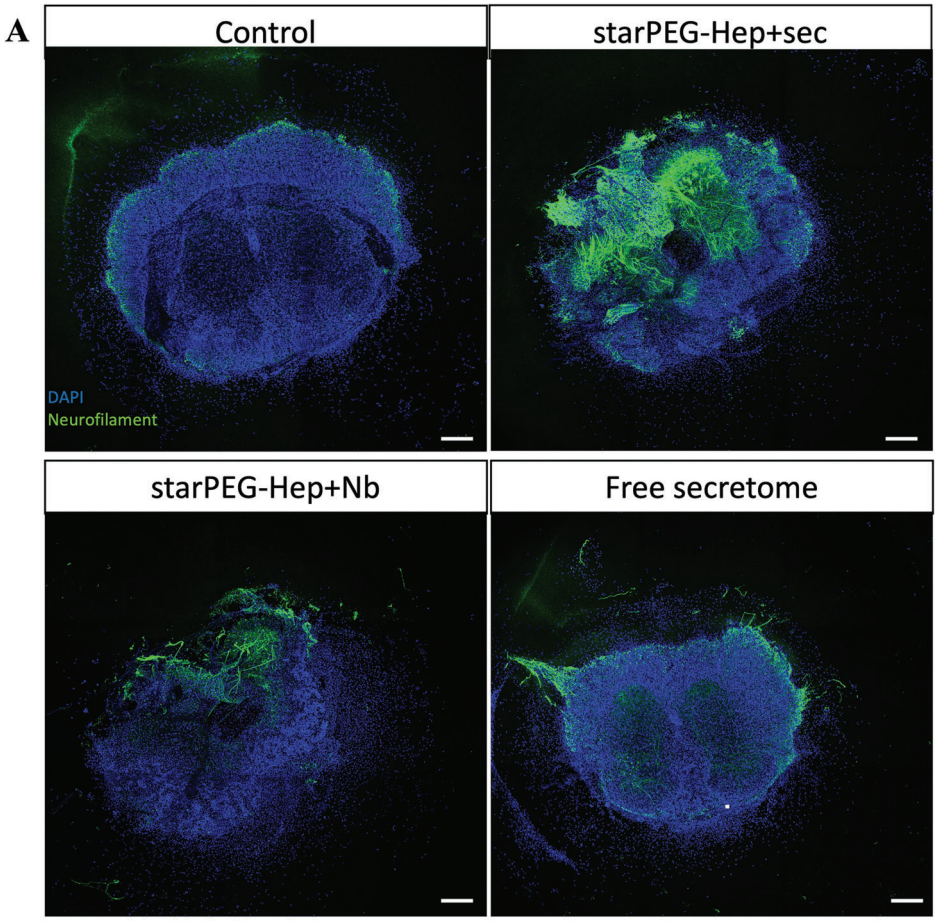

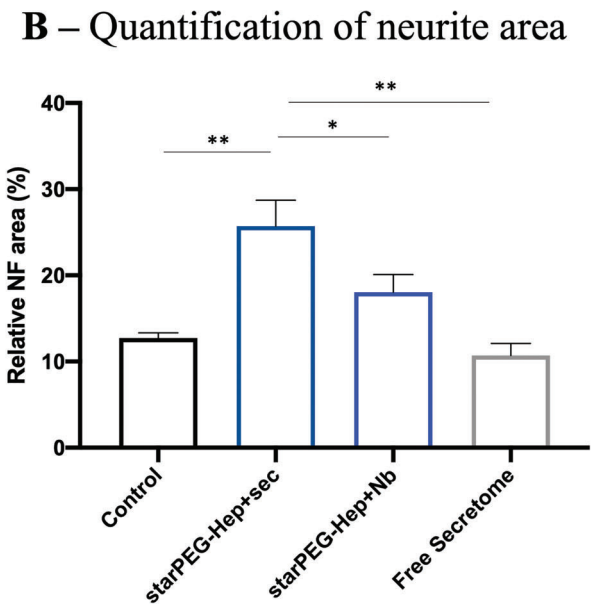

Figure 5. Effect of hASCs secretome released from starPEG-Hep hydrogels in promoting neurite outgrowth in organotypic in vitro cultures. A) Representative micrographs of spinal cord slices when exposed to control, secretome- or vehicle in which secretome was collected (Nb)-loaded starPEG-Hep hydrogels, free secretome conditions. Nuclei were stained with DAPI and neurites with anti-neurofilament. B) Quantification of the percentage of area occupied by neurofilament normalized to total slice area. Results represented four independent experiments with 16/19 replicates. One-way ANOVA; * $p < 0.05$; ** $p < 0.001$. Error bars represent mean ± SEM. Scale bar: 100 µm. DAPI 4′,6′-diamino-2-fenil-indol; NF—Neurofilament.

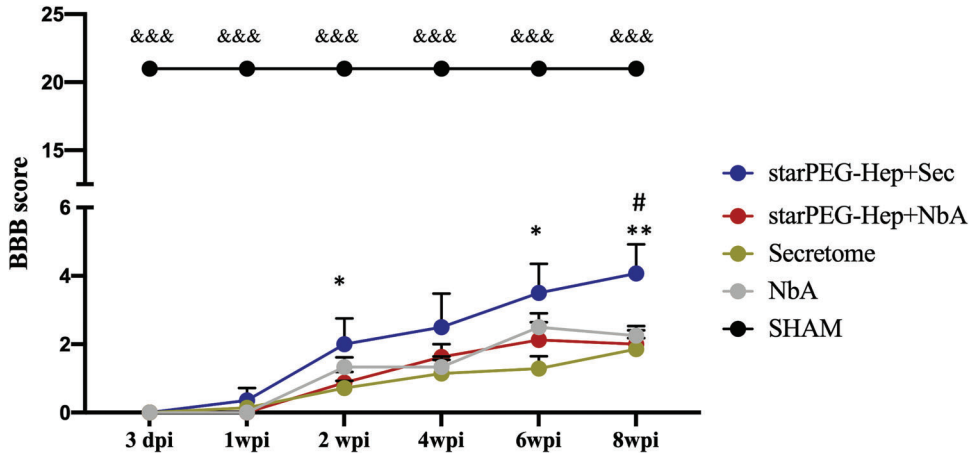

Figure 6. Evaluation of motor performance in SCI rats by BBB test for 8 weeks post-injury. Animals treated with secretome presented improved motor recovery 8 weeks after treatment. Mixed ANOVA; (*) represents differences between starPEG-Hep+sec and Secretome, (#) represents differences between starPEG-Hep+sec versus starPEG-Hep+NbA and NbA, and (&) represents differences between SHAM group and all other; * and # $p < 0.05$; **$p < 0.001$ and &&& $p < 0.0001$. Error bars represent mean ± SEM.

findings from organotypic spinal cord cultures where the free secretome group promoted significantly lower neurite extension (Figure 5). Moreover, all groups presented statistical differences from SHAM animals, as presented in Table S4, Supporting Information.

The BBB score of animals treated with starPEG-Hep+sec indicates that animals could perform extensive movements of two joints (such as ankle, knee, or hip), while animals treated with starPEG-Hep+NbA or NbA were only able to perform extensive movement of one joint and slight movement of the third. Finally, animals treated with secretome only performed slight movements of hindlimbs joints.

2.5. hASCs Secretome Released from starPEG-Hep Hydrogels Decreases the Inflammation in an SCI Model

8 weeks after spinal cord transection, animals were sacrificed and the spinal cords were processed for histological analysis. Neuroinflammation in the tissue was evaluated through immunostaining with Iba-1. In this sense, the area of ameboid microglia, a phenotype associated with higher inflammation, was quantified (**Figure 7**A). Statistical analysis showed that there was a significant effect on Iba-1 staining (F (4.30) = 96.90, $p < 0.0001$). Animals treated with starPEG-Hep+sec presented a significantly reduced area of ameboid microglia ($p = 0.019$) when compared with animals treated with secretome only ($n = 7$; 38.88 ± 7.44 versus $n = 7$; 48.59 ± 5.05) or NbA ($n = 6$; 49.28 ± 4.32; $p = 0.015$; Figure 7C). Previous studies have shown that the starPEG-Hep hydrogels can reduce inflammation by scavenging inflammatory mediators.[81,82] In line with those findings, a slight attenuation of Iba-1 expression was observed in animals treated with starPEG-Hep+NbA, which points to the anti-inflammatory characteristics of the pure hydrogels ($n = 4$; 44.43 ± 7.77, $p = 0.49$) with only the starPEG-Hep+sec effectively attenuating inflammation in the SCI model. All statistical comparisons between groups are presented in Table S5, Supporting Information.

Other markers were used to assess astrocytes (glial fibrillary acidic protein (GFAP)) and axonal regeneration/preservation (NF), which are displayed in Figure S3, Supporting Information. A decrease in the percentage of GFAP positive area at the rostral, epicenter, and caudal regions was also observed in animals treated with starPEG-Hep+sec compared with animals treated with secretome and NbA (Figure S3B, Supporting Information). A similar trend occurs for NF-positive areas. While a slight increase in NF positive area in starPEG-Hep+sec is observed at the epicenter region, a decrease is noticed in rostral and caudal regions with all other groups (Figure S3C, Supporting Information). Nevertheless, no significant differences were observed among treated animals for both markers (Table S6, Supporting Information).

Altogether, these data indicate that motor recovery seems to be favored by a reduced inflammatory response to treatment in local tissue. Furthermore, it has been previously demonstrated that hASCs secretome promoted a reduced inflammatory response in vivo, either by treatment with secretome systemically in mice model[24] or the local cell transplantation.[9,10] Moreover, ASCs secretome can induce M2 polarization through mammalian target of rapamycin complex 1 (mTORC1) and mTORC2 pathways.[83] Other authors also hypothesized that hASCs transplantation in a contusion injury mice model could reduce neuroinflammation by reducing microglia/macrophages at the lesion site, as well as inhibiting Jagged1/Notch pathway.[84] This pathway has been implicated in modulating the immune response after lesion in the central nervous system (CNS) by impacting cell fate decisions and endogenous neurogenesis.[85] On the other hand, interferon gamma (IFN-γ), present in secretome and released by hydrogels, may determine microglia's anti or pro-inflammatory state. Indeed a lower concentration can induce a neuroprotective function.[86,87]

SCI is characterized by an exacerbation of inflammatory response, which could be one of the causes of the massive damage to the tissue after lesion. After we observed an attenuation of inflammation characterized by the reduction of ameboid microglia in the damaged tissue of animals treated with hydrogel and

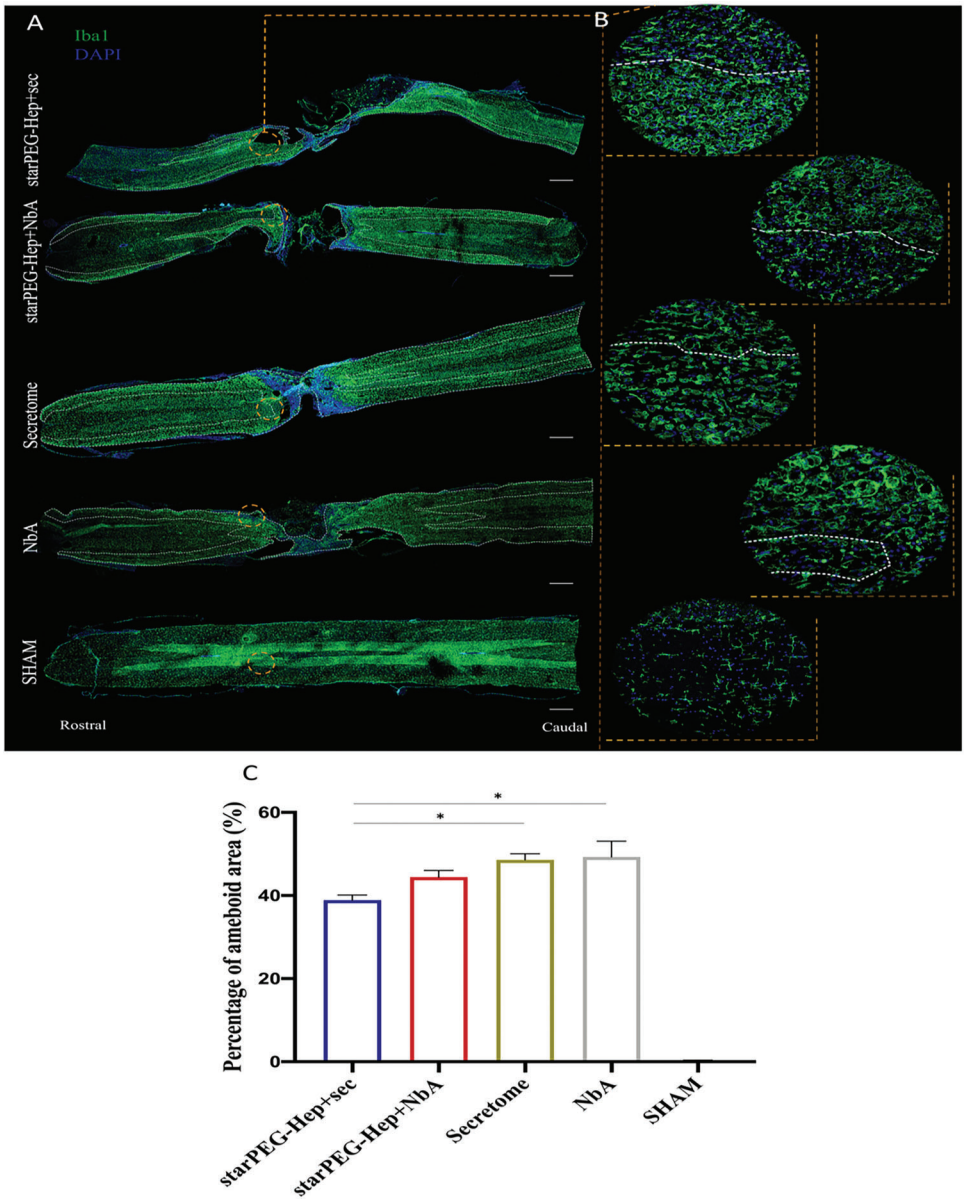

Figure 7. Representative confocal microscopy images of longitudinal sections of spinal cord tissue for Iba1 staining. A) delineated ameboid area in animals treated with starPEG-Hep+sec, starPEG-Hep+NbA, Secretome, NbA, and SHAM 8 weeks after lesion. B) Magnification of tissue stained with anti-Iba1 and considered ameboid area. C) quantification of ameboid area in all groups. Ameboid area was normalized to total area of the tissue and plotted as percentage. One-Way ANOVA, * $p < 0.05$; Error bars represented mean ± SEM. Scale bar: 100 µm.

secretome, we evaluated if the same could be observed systemically. For this purpose, animal serum was collected at three different time points (48 h, 4, and 8 wpi) and the expression of cytokines was evaluated by a cytokine array. Molecular analyses of sera at 48 h post-lesion are presented in **Figure 8**B, where the expression as a heatmap (Figure 8A). Animals treated with starPEG-Hep+sec have an increase in IL-10 compared with animals treated with hydrogel only, secretome, or NbA, and a decrease of inflammatory cytokine monocyte chemoattractant protein (MCP)-1 compared with other groups. Moreover, cluster of differentiation 86 (CD86), a classically (M1) marker, presented values similar to SHAM animals at this time point.

After 4 weeks (Figure 8C and Figure S4A, Supporting Information), animals treated with starPEG-Hep+sec continue to have a higher expression of IL-10 when compared with animals treated with starPEG-Hep+NbA, secretome, or NbA, Figure 8C. Interestingly, at this time point, a decrease in expression of CD86 is observed compared with NbA treated animals. On the other hand, values of MCP-1 remained similar to values obtained at 48 h, with a decrease in groups treated with starPEG-Hep+NbA, secretome, or NbA.

Right before sacrifice (8 weeks, Figure 8D and Figure S4B, Supporting Information), sera analysis revealed an increase in IL-10 levels in animals treated with starPEG-Hep+sec and

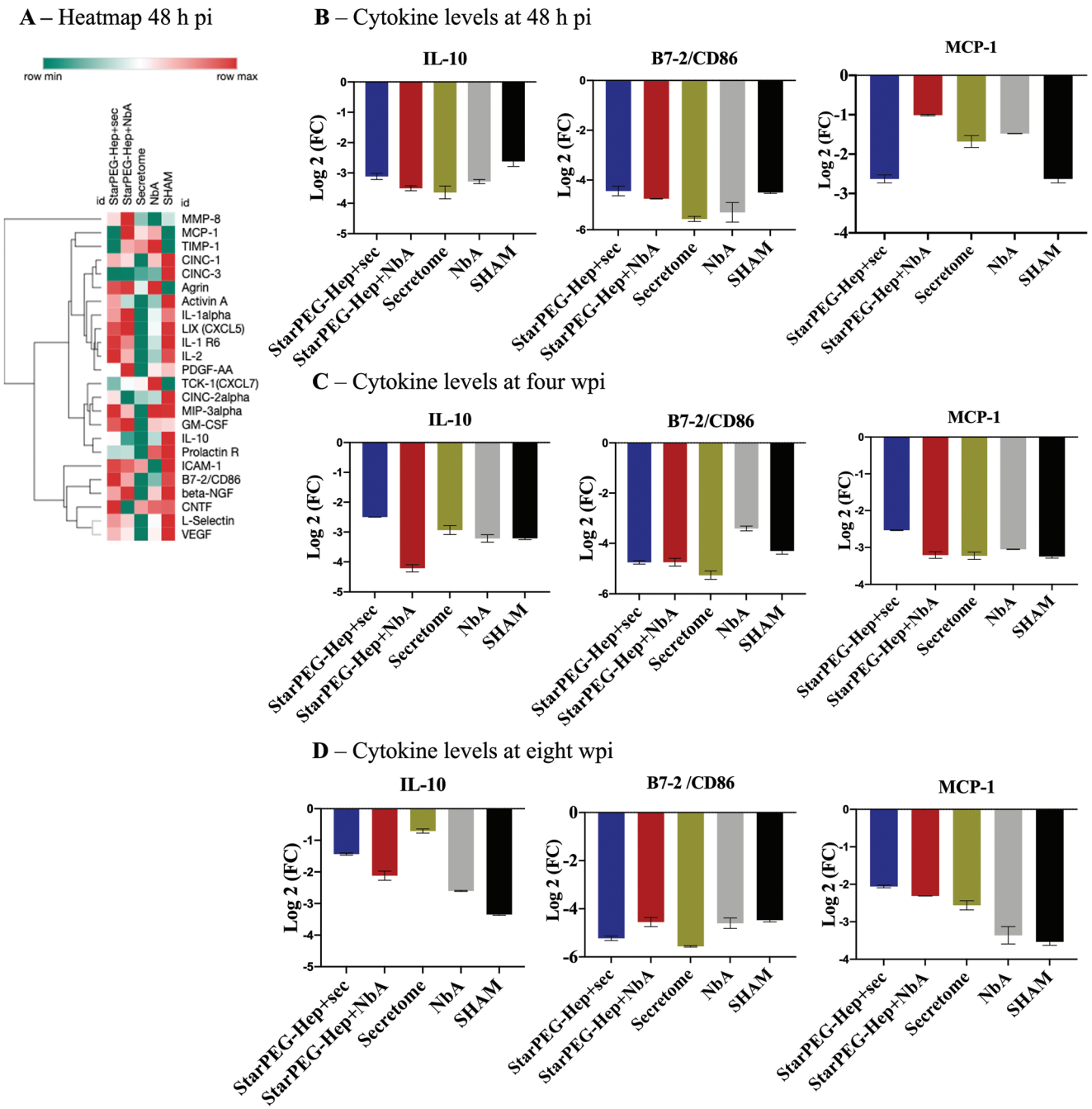

Figure 8. Molecular analysis of collected sera following SCI using Rat Cytokine Array C2 from RayBiotech. A) Representative heat map at 48 h pi of the panel for the different groups was generated using the BROAD Institute's R implementation of Morpheus with Euclidean distance hierarchical clustering. B) Relative expression of selected pro-inflammatory and anti-inflammatory cytokines at 48 h pi, C) 4 wpi, and D) 8 wpi. Data are shown as mean Log2 (fold change—FC) relative to the normalization of each cytokine to the positive controls of each membrane. Error bars represented mean ± SEM.

secretome compared to other groups (Figure 8D). The release of IL-4 or IFN-γ by secretome-loaded hydrogels has been previously shown to induce IL-10 production by microglia/macrophages, leading to increased circulation levels.[88,89] Thus administration of IL-10 has been shown to decrease the levels of pro-inflammatory cytokines and contributed to motor recovery after lesion.[90,91] At the same time, as MCP-1 has been shown to play a critical role in mediating neuron-macrophage interactions that contribute to axonal growth and M2 phenotype polarization, the moderate levels of MCP-1 observed over time may down regulate the inflammatory response and endure the regenerative process.[92] CD86, a marker of M1 phenotype,[93] demonstrated a slight decrease from 4 weeks post-injury and compared with animals treated with hydrogel and NbA at this time point. It is also worth noting that animals treated with starPEG-Hep+sec have higher levels of VEGF expression than all other groups at all time

points, which was shown to inhibit inflammatory response by increasing autophagy contributing to motor improvements after SCI.[94]

Together, the reported data demonstrate for the first time that a biohybrid hydrogel-based sustained hASCs secretome release comprising pro-regenerative cytokines (IL-4, IL-2) and growth factors (BDNF, GDNF). In vitro, hASCs secretome release from starPEG-Hep hydrogel promoted significant hNPCs differentiation in immature (DCX) and mature (MAP2) neurons. Neurite extension was found to be greater in organotypic spinal cord slices if treated with starPEG-Hep+sec. Significant motor recovery in a complete SCI rat model further confirmed the robustness of the delivery system, accompanied by a reduced ameboid microglia area, as well as increased levels of the anti-inflammatory cytokine IL-10 in animal sera.

3. Conclusion

A StarPEG-Hep hydrogel was successfully tuned for sustained hASCs secretome release over weeks as well as for mechanical tissue stabilization to promote neural regeneration.[95,96] The system was demonstrated to be effective in an SCI animal model in reducing inflammation management and initiating pro-regenerative processes. In perspective, the approach may offer unprecedented clinical treatment modalities for SCI.

4. Experimental Section

Synthesis of Hydrogel Precursors, starPEG, Heparin Maleimide: Thiol end-functionalized 4-arm star-PEG (MW 10000, USA) was purchased and maleimide-functionalized heparin (MW 15000, Merck, Germany) was synthesized as previously described.[47] Briefly, heparin (1.5 mM) dissolved in PBS was mixed with an equal volume of starPEG (1.1 to 2.2 mM) to produce hydrogels in the crosslinking range of 0.75–1.5 (molar ratio of starPEG to heparin) (Detailed in Supporting Information).

Rheological Measurements: For rheological measurements, hydrogels with different molar ratios (0.75–1.5) were prepared. Briefly, 67 µL of hydrogel were prepared and allowed to polymerize between two hydrophobic Sigmacote coverslips (Merck, Germany) of defined diameter (D_i = 9 mm). After polymerization, discs were hydrated in PBS. Then, oscillating measurements on swollen gel disks were carried out on a rotational rheometer (ARES LN2; TA Instruments, Germany), with plate-plate geometry (plate diameter 25 mm; gap width, 1.2–1.5 mm). Frequency sweeps were performed at 25 °C with a shear frequency range of 10^{-1}–10^{2} rad s^{-1} and a strain amplitude of 2%. Mean values of the storage modulus were calculated. Experiments were performed in triplicate. The gel volumetric swelling of the gels was determined by the following equation: where d_0 is the diameter of the unswollen gel disk and d is the diameter after swollen gel for 24 h in PBS.

$$Q = \left(\frac{d}{d_0}\right)^3 \quad (1)$$

Mesh Size: The mesh size of a hydrogel was defined as the distance between two entanglement points (ξ) and varied with the different molar ratios in a hydrogel network.[97] It was calculated from the storage modulus G′ based on rubber elasticity theory[56] using the following Equation (2), where G' is the storage modulus, N_A the Avogadro constant, R the molar gas constant, and T the temperature:

$$\xi = \left(\frac{G' N_A}{RT}\right)^{-\frac{1}{3}} \quad (2)$$

Cell Isolation and Culture: The hASCs were obtained from lipoaspirates from consenting donors under a protocol approved and reviewed by an institutional board of LaCell LLC. Cells were isolated according to the previous protocol.[98] The culture conditions of these cells are described in Supporting Information.

Secretome Collection: For secretome collection, hASCs were seeded at a density of 4000 cells cm^{-2} in cell culture flasks with alpha minimum essential medium (α-MEM). The medium was harvested 72 h after culture and the cells were washed four times with PBS without Ca^{2+}/Mg^{2+} (Merk, Germany). The cells were then conditioned for 24 h in Neurobasal medium (ThermoFisher, USA) with 1% penicillin/streptomycin or Neurobasal A (ThermoFisher, USA) with 1% kanamycin, depending on which cultures the secretome will be applied. It was further centrifuged (249 × *g*, Megafuge 1.0R, Heraeus, Germany) for five min to remove any cell debris. Then, hASCs secretome was concentrated (100×) by centrifugation (3000 × *g*) using 5 kDa cut-off concentrator (Vivaspin, GE Healthcare, UK) and frozen at −80 °C until used.

Characterization of Secretome Release by Immunofluorescence: For fluorescence release experiments, secretome was labeled using a FluoReporter FITC protein labeling Kit (ThermoFisher, USA). FITC dye binds to primary amine bonds of proteins forming a dye-protein conjugate, which was detected by fluorescence emission at 518 nm, respectively. Briefly, secretome was labeled according manufacturer's procedures at a labeling ratio of 1:2 protein to dye.

For gel formation, labeled secretome (10 µL) was mixed with heparin (5 µL) and starPEG (5 µL) and allowed to polymerize inside low protein binding tubes. Secretome was allowed to release from hydrogels into PBS supplemented with BSA (1%, 300 µL). Samples from released secretome were collected at defined intervals (0 h, 3 h and 1, 2, 3, 4, 5, 6, 7, 10 days), and replaced by an equal volume of fresh medium. The release samples were stored at −80 °C until analyzed by measuring fluorescence intensity on a Varioskan flash plate reader (ThermoFisher).

Characterization of Secretome Release by Array Membranes: To obtain samples for these experiments, secretome (15 µL) was mixed with heparin (7.5 µL) and then loaded into starPEG (7.5 µL) into 24-well plate. Secretome was allowed to release by adding Neurobasal medium (1 mL, ThermoFisher, USA) supplemented with 1% penicillin/streptomycin (ThermoFisher, USA). Samples were collected at defined time points (2 and 10 days) and replaced by an equal volume of fresh medium. The released samples were stored at −80 °C until analyzed by Human Neuro Discovery Array C1 (C-Series RayBiotech, USA) and Human Cytokine Antibody Array C5 (C-Series RayBiotech, USA).

For secretome analysis, after blocking the membrane for 30 min at RT, released samples (1 mL) were incubated in each well overnight at 4 °C. After washing five times, the membranes were incubated with a biotinylated antibody cocktail for 2 h at RT. Then membranes were incubated with HRP-Streptavidin for 2 h at RT and analyzed by chemiluminescence detection in Sapphire Biomolecular Imager (Azure Biosystems, USA). Analysis of the membranes was performed in AzureSpot Analysis software (Azure Biosystems, USA) where the relative intensity of each spot was measured. Afterward, quantification was done by subtracting the background in each spot and normalizing it to positive control in each membrane.

Neural Progenitor Cells (hNPCs) Growth and Incubation with Released Secretome: To study the potential of secretome released from starPEG-Hep hydrogels in promoting neuronal differentiation hNPCs were used. hNPCs were kindly gifted from Prof. Leo A. Behie (University of Calgary, Canada). Cells were isolated from the telencephalon region of a 10 week post-conception fetus, as described previously.[99] Ethical guidelines were previously established and approved by the Conjoint Health Research Ethics Board (CHREB, University of Calgary, Canada; ID: E-18786). Cells were thawed and cultured as described in Supporting Information. For differentiation assays, neurospheres were mechanically dissociated and plated in 24-well plates in coverslips coated with poly-D-Lysine (100 µg mL^{-1}; Merk, USA) and laminin (10 µg mL^{-1}; Merk, USA) using 60 000 cells per well. For these experiments, 24-HTS Transwell plates (Costar, Corning, USA) were used. After seeding hNPCs on the bottom, hydrogels were prepared and pipetted onto the insert membrane. Neurobasal-A supplemented with 1% kanamycin and 1% GlutaMAX (Gibco, USA) (basal medium) was added as

a negative control, and the same amount of loaded secretome was diluted in this medium added as a free condition. Additionally, Neurobasal-A supplemented with B27 (2%, ThermoFisher, USA), FGF-2 (0.05%; R&D Systems, USA), kanamycin (1%), and GlutaMAX (1%) was used as a positive control. Cultures were maintained for 5 days.

Spinal Cord Slices Isolation and Incubation with Released Secretome: Organotypic spinal cord slice cultures were prepared from Wistar Han rats as described in Supporting Information. Then, viable slices were deposited on top of collagen drops (30 µL). Additionally, drops starPEG hydrogel loading secretome (30 µL) were allowed to polymerize and release secretome in the same well. Afterward, Neurobasal medium supplemented with B27 (2%, ThermoFisher, USA), glucose (2%, 300 mg) (Merck, USA), L-Glutamine (1%, ThermoFisher, USA), and 1% pen/strep was added to each well and medium changed after 2 days and the cultures were maintained at 37 °C and 5% CO_2 for 7 days.

ICC: ICC was used to evaluate neuronal differentiation of hNPCs, as well as to identify neurite projections in spinal cord slices. Rabbit anti-doublecortin (DCX, 1:300 Abcam, UK) and mouse anti-microtubule associated protein-2 (MAP-2, 1:500, Merck, USA) were used to unveil neuronal differentiation of hNPCs for immature and mature neurons, respectively. Mouse anti-NF (NF, 1:200; Merck, USA) to identify neurites in spinal cord slices. Imaging was performed with a fluorescence microscope (BX61, Olympus, Germany) for hNPCS and with a confocal point-scanning microscope Olympus FV1000 for spinal cord slices. A detailed protocol can be founded in Supporting Information

Neuronal Differentiation Analysis: Cell counts were performed under blinded conditions using Image J (NIH) software for quantification. Ten representative fields per condition were selected and analyzed. The number of positive cells for DCX and MAP-2 were counted per field and normalized to a total number of cells in each field stained with DAPI. Results were presented as a percentage of differentiated cells.

Neurite Extension Analysis: To quantify the area occupied by neurites, Fiji software was used. First, the scale was defined and the total slice area was measured, using the proper drawing tools. Then applying the threshold contrast was possible to emphasize the neurite identification. Using the function "Analyze particles," the total area occupied by neurite was calculated. The results were then normalized to the total area of the slice and presented as a percentage of neurite area.

Study Design: The final goal of this study was to evaluate the capacity of a secretome release system based on the use of starPEG-Hep hydrogel in promoting regeneration in an SCI animal model. Thus, regenerative processes were assessed by functional recovery and histological alterations. Animals were randomly treated and all data collection (behavior and histology) was obtained in blinded conditions. All procedures were carried out in accordance with EU directive 2010/63/EU and were approved by the ethical committee in life and health sciences (ID: SECVS116/2016, University of Minho, Braga, Portugal).

Animals and Groups: In this in vivo study, Wistar Han female rats (8–11 weeks old, weighing 170–190 g) were used. Animals were kept in light and temperature-controlled cages and fed ad libitum with a standard diet. The handling of the animals was carried out 5 days before the surgery. The animals were divided into five different groups according to the treatment/procedure instituted: 1) Animals subjected to SCI that were injected with starPEG-Hep+sec ($n = 7$); 2) SCI animals treated with starPEG-Hep+NbA ($n = 4$); or 3) SCI animals treated with secretome locally ($n = 7$); 4) SCI animals treated only with NbA ($n = 6$); and 5) Animals with laminectomy only, SHAM ($n = 7$).

SCI Surgery: For surgery, animals were previously anesthetized with an intraperitoneal injection of a mixture (1.5:1) of ketamine (100 mg mL^{-1}, Ketamidor/Richter Pharma, Austria) and medetomidine hydrochloride (1 mg mL^{-1}, Seedorm/ProdivetZN, Portugal). After anesthesia, the animals' fur was shaved and the skin was disinfected with 70% ethanol and chlorhexidine. The incision was made in the dorsal midline, between T7 and T13, with subsequent retraction of the paravertebral muscles. A laminectomy (removal of the spinous processes to expose the spinal cord) was performed at the T8 level and a total spinal cord transection was performed at this level. After administering the respective treatment, the paravertebral muscles and the skin were sutured with Vicryl sutures (Johnson and Johnson, USA). After surgery, all rats were kept under heat lamps and received daily post-operative care (protocol described in Supporting Information)

Hydrogel Preparation: For in vivo application heparin, starPEG and RGD (990 g mol^{-1}, Peptides International) were dissolved as previously described and filtered using low protein binding 0.2 µm filter (Acrodisc, PALL, USA) to ensure sterile conditions of the materials prior to injecting. Briefly, hASCs secretome (5 µL collected in NbA) was mixed with an equal amount of heparin/RGD and starPEG (2.5 µL).

Locomotor Rating: The BBB locomotor rating scale[100] was employed to evaluate motor behavior and recovery. The test was performed for 4 min by two blinded researchers starting 3 days after surgery and performed 1, 2, 4, and 6 weeks up to 8 weeks. Locomotion of the affected hindlimbs was rated in a score of 0 if no movement was observed, 1 to 8 indicates some movement of joints without weight support. 9 to 20 animals were capable of weight support, had coordinated steps and trunk stability, and finally, a 21 score corresponds to a normal animal with perfect movements. To attribute the final score to each animal, the average score of both hindlimbs was made and plotted over 8 weeks of behavior analysis.

Immunohistochemistry: 8 weeks post-injury, rats were deeply anesthetized by an intraperitoneal injection of sodium pentobarbital (200 mg mL^{-1}, Eutasol, Ecuphar, Spain) and perfused through the ascending aorta with NaCl (0.9%; 100 mL) followed by PFA (4%; 100 mL) After tissue preparation the following primary antibodies were used: rabbit anti-rat GFAP for astrocytes (1:200, Dako, Denmark), mouse anti-NF (NF, 1:200, Merck, USA), rabbit anti-Iba-1 (1:1000, Wako, Japan). Finally, the slides were observed at a fluorescence microscope, Olympus Widefield Inverted Microscope IX81. All images were treated using Fiji software. Detailed protocols of tissue preparation, immunohistochemistry, and staining quantification are presented in Supporting Information.

Serum Collection and Analysis by Neuro Array Membrane: Rat blood was collected directly from the tail vein at 48 h and 4 weeks post-injury and from the heart at sacrifice. Blood was allowed to coagulate for ≈15 min and centrifuged at 15 330 × *g* for 15 min. Serum was collected and stored at −80 °C until further use. For each group, a pool of serum was made and analyzed using Rat Cytokine Array C2 (C-Series RayBiotech, USA) according to the manufactures instructions or as explained previously. Analysis of the membranes was performed in AzureSpot Analysis software (Azure Biosystems, USA), where the relative intensity of each spot was measured. Afterward, to quantify the relative intensity of each spot corresponding to a different protein, the background was subtracted and intensity was normalized to positive controls.

Statistical Analysis: Data regarding neurodifferentiation of hNPCs and BBB test were analyzed using Mixed ANOVA to compare the mean values of five groups. When evaluating the neurite outgrowth in spinal cord slices, ameboid area of Iba-1 and positive area of NF and GFAP one-way ANOVA were performed. A pairwise comparison between groups based on estimated marginal means using Turkey's correction was performed. The significance value was set as $p \leq 0.05$ for all statistical tests and graphs were presented as mean ± SEM. For all data, normality was assessed using Shapiro-Wilk statistical tests and taking into account the measures of skewness and kurtosis. Moreover, it was important to highlight that ANOVA distribution can be approximately normally distributed for repeated measurements.[101] IBM SPSS statistics version 27 for IOS (IBM Co., USA) was used to perform all statistical analyses. GraphPad Prism ver.8.4.3 (GraphPad Software, La Jolla, USA) was used for graphical representations.

Supporting Information

Supporting Information is available from the Wiley Online Library or from the author.

Acknowledgements

This work was supported by the Prémios Santa Casa Neurociências–Prize Melo e Castro for Spinal Cord Injury Research (MC-04/17; MC-18-2021)

and the Portuguese Foundation for Science and Technology (Ph.D. fellowship to D.S. (PD/BDE/135567/2018 and COVID/BDE/152051/2022); T.S.P. (PD/BDE/143150/2019); J.R.C. (SFRH/BD/145860/2019); J.A. (2021.08337.BD); S.B.-A. ((PD/BDE/135568/2018). This work was funded by national funds and FEDER, through the Foundation for Science and Technology (FCT), under the scope of the projects UIDB/50026/2020; UIDP/50026/2020; POCI-01-0145-FEDER-029206; POCI-01-0145-FEDER-031392; PTDC/MED-NEU/31417/2017; NORTE-01-0145-FEDER-029968; POCI-01-0145-FEDER-029751; POCI-01-0145-FEDER-032619. This work was also funded by ICVS Scientific Microscopy Platform, a member of the national infrastructure PPBI—Portuguese Platform of Bioimaging (PPBI-POCI-01-0145-FEDER-022122. This work was developed under the scope of the project NORTE-01-0145- FEDER-000013 and NORTE-01-0145-FEDER-000023, supported by the Northern Portugal Regional Operational Programme (NORTE 2020), under the Portugal 2020 Partnership Agreement, through the European Regional Development Fund (FEDER). This work also received support from the Portuguese Foundation for Science and Technology (FCT): projects UID/FIS/04650/2020, PTDC/EMD-EMD/28159/2017, and PTDC/BTM-MAT/28237/2017. Dr. Jeff Gimble and LaCell, Inc. kindly provided the adipose tissue-derived stem cells used in this study. The authors thank Nelly Rein for her technical advice and support in working with the hydrogel material.

Conflict of Interest

The authors declare no conflict of interest.

Author Contributions

C.W. and A.J.S. share senior authorship. D.S. designed and performed most of the experiments, collected and analyzed the data, and drafted the manuscript. T.S.P., J.R.C., R.L., J.A., S.B.-A., C.R.M., and J.D. helped in vitro and animal experiments. L.S. and P.A. helped in designing experiments. U.F. and C.W. provided hydrogel materials. A.J.S. conceived and financially supported the study, and participated in its design and coordination. L.S., U.F., C.W., and A.J. S. critically read the manuscript. U.F., R.A.S., C.W., and A.J.S. supervised the study. All authors read and approved the final manuscript.

Data Availability Statement

The data that support the findings of this study are available from the corresponding author upon reasonable request.

Keywords

delivery systems, heparin, hydrogels, secretome, spinal cord injury, star-shaped poly (ethylene glycol)

Received: October 31, 2022
Revised: February 6, 2023
Published online: March 4, 2023

[1] L. Anderberg, H. Aldskogius, A. Holtz, *Upsala J. Med. Sci.* **2007**, *112*, 259.
[2] N. Level, *J. Spinal Cord Med.* **2018**, *30*, 304.
[3] S. Huh, H. Y. Ko, *Spinal Cord* **2020**, *58*, 998.
[4] K. D. Anderson, *J. Neurotrauma* **2004**, *21*, 1371.
[5] M. D. Norenberg, J. Smith, A. Marcillo, *J. Neurotrauma* **2004**, *21*, 429.
[6] J. W. Rowland, G. W. J. Hawryluk, B. Kwon, M. G. Fehlings, *Neurosurg. Focus* **2008**, *25*, E2.
[7] A. Anjum, M. D. Yazid, M. F. Daud, J. Idris, A. M. Hwei Ng, A. S. Naicker, O. H. Rashidah Ismail, R. K. A. Kumar, Y. Lokanathan, *Int. J. Mol. Sci.* **2020**, *21*, 7533.
[8] A. P. Tran, P. M. Warren, J. Silver, *Physiol. Rev.* **2018**, *98*, 881.
[9] E. D. Gomes, S. S. Mendes, R. C. Assunção-Silva, F. G. Teixeira, A. O. Pires, S. I. Anjo, B. Manadas, H. Leite-Almeida, J. M. Gimble, N. Sousa, A. C. Lepore, N. A. Silva, A. J. Salgado, *Stem Cells* **2018**, *36*, 696.
[10] Z. Zhou, X. Tian, B. Mo, H. Xu, L. Zhang, L. Huang, S. Yao, Z. Huang, Y. Wang, H. Xie, L. Xu, H. Zhang, *Stem Cell Res. Ther.* **2020**, *11*, 212.
[11] M. Bydon, A. B. Dietz, S. Goncalves, F. M. Moinuddin, M. A. Alvi, A. Goyal, Y. Yolcu, C. L. Hunt, K. L. Garlanger, A. S. Del Fabro, R. K. Reeves, A. Terzic, A. J. Windebank, W. Qu, *Mayo Clin. Proc.* **2020**, *95*, 406.
[12] J. Vaquero, M. Zurita, M. A. Rico, C. Bonilla, C. Aguayo, J. Montilla, S. Bustamante, J. Carballido, E. Marin, F. Martinez, A. Parajon, C. Fernandez, L. D. Reina, *Cytotherapy* **2016**, *18*, 1025.
[13] A. J. Braga Osorio Gomes Salgado, R. L. Goncalves Reis, N. Jorge Carvalho Sousa, J. M. Gimble, A. J. Salgado, R. L. Reis, N. Sousa, *Curr. Stem Cell Res. Ther.* **2010**, *5*, 103.
[14] S. Lu, C. Lu, Q. Han, J. Li, Z. Du, L. Liao, R. C. Zhao, *Toxicology* **2011**, *279*, 189.
[15] S. K. Kang, E. S. Jun, Y. C. Bae, J. S. Jung, *Dev. Brain Res.* **2003**, *145*, 141.
[16] E. D. Gomes, S. S. Mendes, H. Leite-Almeida, J. M. Gimble, R. Y. Tam, M. S. Shoichet, N. Sousa, N. A. Silva, A. J. Salgado, *Biomaterials* **2016**, *105*, 38.
[17] E. D. Gomes, B. Ghosh, R. Lima, M. Goulão, T. Moreira-Gomes, J. Martins-Macedo, M. W. Urban, M. C. Wright, J. M. Gimble, N. Sousa, N. A. Silva, A. C. Lepore, A. J. Salgado, *Front. Bioeng Biotechnol.* **2020**, *8*, 984.
[18] F. Cofano, M. Boido, M. Monticelli, F. Zenga, A. Ducati, A. Vercelli, D. Garbossa, *Int. J. Mol. Sci.* **2019**, *20*, 2698.
[19] M. I. Guillén, J. Platas, M. D. Pérez del Caz, V. Mirabet, M. J. Alcaraz, *Front. Physiol.* **2018**, *9*, 661.
[20] C. A. Ribeiro, J. S. Fraga, M. Grãos, N. M. Neves, R. L. Reis, J. M. Gimble, N. Sousa, A. J. Salgado, *Stem Cell Res. Ther.* **2012**, *3*, 18.
[21] S. C. Serra, J. C. Costa, R. C. Assunção-Silva, F. G. Teixeira, N. A. Silva, S. I. Anjo, B. Manadas, J. M. Gimble, L. A. Behie, A. J. Salgado, *Biochimie* **2018**, *155*, 119.
[22] R. C. Assunção-Silva, B. Mendes-Pinheiro, P. Patrício, L. A. Behie, F. G. Teixeira, L. Pinto, A. J. Salgado, *Biochimie* **2018**, *155*, 83.
[23] L. A. Rocha, E. D. Gomes, J. L. Afonso, S. Granja, F. Baltazar, N. A. Silva, M. S. Shoichet, R. A. Sousa, D. A. Learmonth, A. J. Salgado, *Front. Cell Dev. Biol.* **2020**, *8*, 489.
[24] A. G. Pinho, J. R. Cibrão, R. Lima, E. D. Gomes, S. C. Serra, J. Lentilhas-Graça, C. Ribeiro, S. Lanceros-Mendez, F. G. Teixeira, S. Monteiro, N. A. Silva, A. J. Salgado, *Exp. Neurol.* **2022**, *351*, 113989.
[25] C. A. Bowers, B. Kundu, G. W. J. Hawryluk, *Neural Regener. Res.* **2016**, *11*, 882.
[26] K. A. Follett, R. L. Boortz-Marx, J. M. Drake, S. DuPen, S. J. Schneider, M. S. Turner, R. J. Coffey, *Anesthesiology* **2004**, *100*, 1582.
[27] J. R. W. Kestle, H. J. Hoffman, D. Soloniuk, R. P. Humphreys, J. M. Drake, E. B. Hendrick, *Child's Nerv. Syst.* **1993**, *9*, 163.
[28] Z. Gong, D. Lei, C. Wang, C. Yu, K. Xia, J. Shu, L. Ying, J. Du, J. Wang, X. Huang, L. Ni, C. Wang, J. Lin, F. Li, Z. You, C. Liang, *ACS Biomater. Sci. Eng.* **2020**, *6*, 6331.
[29] J. Pan, J. Deng, Y. Luo, L. Yu, W. Zhang, X. Han, Z. You, Y. Liu, *Stem Cells Dev.* **2019**, *28*, 1620.
[30] L. Zeng, J. He, Y. Cao, J. Wang, Z. Qiao, X. Jiang, L. Hou, J. Zhang, *Smart Polym. Mater. Biomed. Appl.* **2021**, *2*, 229.
[31] R. Shultz, Y. Zhong, *Neural Regener. Res.* **2021**, *16*, 247.

[32] J. Piantino, J. A. Burdick, D. Goldberg, R. Langer, L. I. Benowitz, *Exp. Neurol.* **2006**, *201*, 359.
[33] B. Ghosh, J. Nong, Z. Wang, M. W. Urban, N. M. Heinsinger, V. A. Trovillion, M. C. Wright, A. C. Lepore, Y. Zhong, *Neurobiol. Dis.* **2019**, *127*, 591.
[34] H. L. Xu, F. R. Tian, J. Xiao, P. P. Chen, J. Xu, Z. L. Fan, J. J. Yang, C. T. Lu, Y. Z. Zhao, *Int. J. Nanomed.* **2018**, *13*, 681.
[35] D. Silva, R. A. Sousa, A. J. Salgado, *Mater. Today Bio* **2021**, *9*, 100093.
[36] V. Estrada, N. Brazda, C. Schmitz, S. Heller, H. Blazyca, R. Martini, H. W. Müller, *Neurobiol. Dis.* **2014**, *67*, 165.
[37] L. T. A. Hong, Y. M. Kim, H. H. Park, D. H. Hwang, Y. Cui, E. M. Lee, S. Yahn, J. K. Lee, S. C. Song, B. G. Kim, *Nat. Commun.* **2017**, *8*, 1.
[38] J. A. Burdick, K. S. Anseth, *Biomaterials* **2002**, *23*, 4315.
[39] C. C. Lin, K. S. Anseth, *Pharm. Res.* **2009**, *26*, 631.
[40] K. J. Lampe, D. S. Kern, M. J. Mahoney, K. B. Bjugstad, *J. Biomed. Mater. Res., Part A* **2011**, *96 A*, 595.
[41] U. Freudenberg, A. Hermann, P. B. Welzel, K. Stirl, S. C. Schwarz, M. Grimmer, A. Zieris, W. Panyanuwat, S. Zschoche, D. Meinhold, A. Storch, C. Werner, *Biomaterials* **2009**, *30*, 5049.
[42] A. Zieris, K. Chwalek, S. Prokoph, K. R. Levental, P. B. Welzel, U. Freudenberg, C. Werner, *J. Controlled Release* **2011**, *156*, 28.
[43] U. Freudenberg, J.-U. Sommer, K. R. Levental, P. B. Welzel, A. Zieris, K. Chwalek, K. Schneider, S. Prokoph, M. Prewitz, R. Dockhorn, C. Werner, *Adv. Funct. Mater.* **2012**, *22*, 1391.
[44] I. Capila, R. J. Linhardt, *Angew. Chem., Int. Ed.* **2002**, *41*, 390.
[45] A. Zieris, S. Prokoph, K. R. Levental, P. B. Welzel, M. Grimmer, U. Freudenberg, C. Werner, *Biomaterials* **2010**, *31*, 7985.
[46] L. Schirmer, P. Atallah, C. Werner, U. Freudenberg, *Adv. Healthcare Mater.* **2016**, *5*, 3157.
[47] M. V. Tsurkan, K. Chwalek, S. Prokoph, A. Zieris, K. R. Levental, U. Freudenberg, C. Werner, *Adv. Mater.* **2013**, *25*, 2606.
[48] U. Freudenberg, Y. Liang, K. L. Kiick, C. Werner, *Adv. Mater.* **2016**, *28*, 8861.
[49] U. Freudenberg, A. Zieris, K. Chwalek, M. V. Tsurkan, M. F. Maitz, P. Atallah, K. R. Levental, S. A. Eming, C. Werner, *J. Controlled Release* **2015**, *220*, 79.
[50] P. Atallah, L. Schirmer, M. Tsurkan, Y. D. Putra Limasale, R. Zimmermann, C. Werner, U. Freudenberg, *Biomaterials* **2018**, *181*, 227.
[51] R. D. Bartlett, D. Eleftheriadou, R. Evans, D. Choi, J. B. Phillips, *Biomaterials* **2020**, *258*, 120303.
[52] A. P. Balgude, X. Yu, A. Szymanski, R. V. Bellamkonda, *Biomaterials* **2001**, *22*, 1077.
[53] Z. Z. Khaing, A. Ehsanipour, C. P. Hofstetter, S. K. Seidlits, *Cells Tissues Organs* **2016**, *202*, 67.
[54] M. C. Jimenez Hamann, E. C. Tsai, C. H. Tator, M. S. Shoichet, *Exp. Neurol.* **2003**, *182*, 300.
[55] P. V. Turner, T. Brabb, C. Pekow, M. A. Vasbinder, *J. Am. Assoc. Lab. Anim. Sci.* **2011**, *50*, 600.
[56] M. Rubinstein, R. H. Colby, *Polymer Physics*, Oxford University Press, Oxford **2003**.
[57] J. E. Springer, R. D. Azbill, S. E. Kennedy, J. George, J. W. Geddes, *J. Neurochem.* **1997**, *69*, 1592.
[58] R. Vawda, A. Badner, J. Hong, M. Mikhail, R. Dragas, K. Xhima, A. Jose, M. G. Fehlings, *Stem Cells Dev.* **2020**, *29*, 1429.
[59] A. O. Pires, B. Mendes-Pinheiro, F. G. Teixeira, S. I. Anjo, S. Ribeiro-samy, E. D. Gomes, S. C. Serra, N. A. Silva, B. Manadas, A. J. Salgado, *Stem Cells Dev.* **2016**, *25*, 1073.
[60] R. P. Huang, W. Yang, D. Yang, L. Flowers, I. R. Horowitz, X. Cao, R. Huang, *Expert Opin. Ther. Targets* **2005**, *9*, 601.
[61] U. Freudenberg, P. Atallah, Y. D. P. Limasale, C. Werner, *Faraday Discuss.* **2019**, *219*, 244.
[62] H. L. Xu, F. R. Tian, C. T. Lu, J. Xu, Z. L. Fan, J. J. Yang, P. P. Chen, Y. D. Huang, J. Xiao, Y. Z. Zhao, *Sci. Rep.* **2016**, *6*,38332.
[63] J. Langhnoja, L. Buch, P. Pillai, *Cell Biol. Int.* **2021**, *45*, 432.
[64] S. Q. Chen, Q. Cai, Y. Y. Shen, X. Y. Cai, H. Y. Lei, *Int. J. Dev. Neurosci.* **2014**, *38*, 74.
[65] A. M. Nicaise, K. M. Johnson, C. M. Willis, R. M. Guzzo, S. J. Crocker, *Mol. Neurobiol.* **2019**, *56*, 3380.
[66] C. A. Ribeiro, A. J. Salgado, J. S. Fraga, N. A. Silva, R. L. Reis, N. Sousa, *J. Tissue Eng. Regener. Med.* **2011**, *5*, 668.
[67] S. A. Eming, T. A. Wynn, P. Martin, *Science* **2017**, *1356*, 1026.
[68] N. G. Frangogiannis, in *Inflammation: From Molecular and Cellular Mechanisms to the Clinic* (Eds: J.-M. Cavaillon, M. Singer), John Wiley And Sons, Weinheim **2017**, pp. 1517–1538.
[69] L. I. Benowitz, P. G. Popovich, *Curr. Opin. Neurol.* **2011**, *24*, 577.
[70] L. F. Martins, R. O. Costa, J. R. Pedro, P. Aguiar, S. C. Serra, F. G. Teixeira, N. Sousa, A. J. Salgado, R. D. Almeida, *Sci. Rep.* **2017**, *7*, 4153.
[71] P. Lu, L. L. Jones, M. H. Tuszynski, *Exp. Neurol.* **2005**, *191*, 344.
[72] L. Crigler, R. C. Robey, A. Asawachaicharn, D. Gaupp, D. G. Phinney, *Exp. Neurol.* **2006**, *198*, 54.
[73] K. M. Keefe, I. S. Sheikh, G. M. Smith, *Int. J. Mol. Sci.* **2017**, *18*, 548.
[74] H. J. Lee, J. S. Ryu, P. J. Vig, *Ther. Delivery* **2019**, *10*, 251.
[75] D. Hakkoum, L. Stoppini, D. Muller, *J. Neurochem.* **2007**, *100*, 747.
[76] F. Y. H. Teng, B. L. Tang, *J. Neurochem.* **2006**, *96*, 1501.
[77] S. Prokoph, E. Chavakis, K. R. Levental, A. Zieris, U. Freudenberg, S. Dimmeler, C. Werner, *Biomaterials* **2012**, *33*, 4792.
[78] M. Zhang, N. Mal, M. Kiedrowski, M. Chacko, A. T. Askari, Z. B. Popovic, O. N. Koc, M. S. Penn, *FASEB J.* **2007**, *21*, 3197.
[79] M. Chudickova, I. Vackova, L. M. Urdzikova, P. Jancova, K. Kekulova, M. Rehorova, K. Turnovcova, P. Jendelova, S. Kubinova, *Int. J. Mol. Sci.* **2019**, *20*, 4516.
[80] T. Cheriyan, D. J. Ryan, J. H. Weinreb, J. Cheriyan, J. C. Paul, V. Lafage, T. Kirsch, T. J. Errico, *Spinal Cord* **2014**, *52*, 588.
[81] N. Lohmann, L. Schirmer, P. Atallah, E. Wandel, R. A. Ferrer, C. Werner, J. C. Simon, S. Franz, U. Freudenberg, *Sci. Transl. Med.* **2017**, *9*, 9044.
[82] L. Schirmer, P. Atallah, U. Freudenberg, C. Werner, *Adv. Sci.* **2021**, *8*, 2170114.
[83] L. Souza-Moreira, V. C. Soares, S. Dias, P. T. Bozza, *Sci. Rep.* **2019**, *9*, 20304.
[84] W. Liu, R. Li, J. Yin, S. Guo, Y. Chen, H. Fan, G. Li, Z. Li, X. Li, X. Zhang, X. He, C. Duan, *J. Neuroinflammation* **2019**, *16*, 8.
[85] X. Z. Hao, L. K. Yin, J. Q. Tian, C. C. Li, X. Y. Feng, Z. W. Yao, M. Jiang, Y. M. Yang, *Front. Cell. Neurosci.* **2018**, *12*, 245.
[86] I. Shaked, D. Tchoresh, R. Gersner, G. Meiri, S. Mordechai, X. Xiao, R. P. Hart, M. Schwartz, *J. Neurochem.* **2005**, *92*, 997.
[87] O. Butovsky, Y. Ziv, A. Schwartz, G. Landa, A. E. Talpalar, S. Pluchino, G. Martino, M. Schwartz, *Mol. Cell. Neurosci.* **2006**, *31*, 149.
[88] R. Lima, S. Monteiro, J. Lopes, P. Barradas, N. Vasconcelos, E. Gomes, R. Assunção-Silva, F. Teixeira, M. Morais, N. Sousa, A. Salgado, N. Silva, *Pharmaceuticals* **2017**, *10*, 83.
[89] H. Ishii, S. Tanabe, M. Ueno, T. Kubo, H. Kayama, S. Serada, M. Fujimoto, K. Takeda, T. Naka, T. Yamashita, *Cell Death Dis.* **2013**, *4*, e710.
[90] Z. Zhou, X. Peng, R. Insolera, D. J. Fink, M. Mata, *Exp. Neurol.* **2009**, *220*, 183.
[91] D. J. Hellenbrand, K. A. Reichl, B. J. Travis, M. E. Filipp, A. S. Khalil, D. J. Pulito, A. V. Gavigan, E. R. Maginot, M. T. Arnold, A. G. Adler, W. L. Murphy, A. S. Hanna, *J. Neuroinflammation* **2019**, *16*, 93.
[92] M. J. Kwon, H. Y. Shin, Y. Cui, H. Kim, A. H. Le Thi, J. Y. Choi, E. Y. Kim, D. H. Hwang, B. G. Kim, *J. Neurosci.* **2015**, *35*, 15934.
[93] X. Q. Su, X. Y. Wang, F. T. Gong, M. Feng, J. J. Bai, R. R. Zhang, X. Q. Dang, *Brain Res. Bull.* **2020**, *158*, 1.

[94] H. Wang, Y. Wang, D. Li, Z. Liu, Z. Zhao, D. Han, Y. Yuan, J. Bi, X. Mei, *Biochem. Biophys. Res. Commun.* **2015**, *464*, 453.
[95] N. A. Silva, A. J. Salgado, R. A. Sousa, J. T. Oliveira, A. J. Pedro, H. Leite-Almeida, R. Cerqueira, A. Almeida, F. Mastronardi, J. F. Mano, N. M. Neves, N. Sousa, R. L. Reis, *Tissue Eng., Part A* **2010**, *16*, 45.
[96] K. H. Sitoci-Ficici, M. Matyash, O. Uckermann, R. Galli, E. Leipnitz, R. Later, C. Ikonomidou, M. Gelinsky, G. Schackert, M. Kirsch, *Acta Neurochir.* **2018**, *160*, 449.
[97] Q. Chai, Y. Jiao, X. Yu, *Gels* **2017**, *3*, 6.
[98] S. G. Dubois, E. Z. Floyd, S. Zvonic, G. Kilroy, X. Wu, S. Carling, Y. D. C. Halvorsen, E. Ravussin, J. M. Gimble, *Methods Mol. Biol.* **2008**, *449*, 69.
[99] F. G. Teixeira, K. M. Panchalingam, S. I. Anjo, B. Manadas, R. Pereira, N. Sousa, A. J. Salgado, L. A. Behie, *Stem Cell Res. Ther.* **2015**, *6*, 133.
[100] D. M. Basso, M. S. Beattie, J. C. Bresnahan, *J. Neurotrauma* **1995**, *12*, 1.
[101] Laerd Statistics, https://statistics.laerd.com/spss-tutorials/one-way-anova-repeated-measures-using-spss-statistics.php, accessed: January 2022.